Magnetic and thermal properties of nanoscale heavy-fermion particles

P. Schlottmann
Department of Physics, Florida State University, Tallahassee, Florida 32306

(Received 15 June 2001; revised manuscript received 13 August 2001; published 19 December 2001)

The heavy-fermion state in some rare-earth and actinide compounds arises from a hybridization of extended conduction states with strongly correlated localized *f* states. The properties of the heavy fermions are those of a Fermi liquid with small Fermi energy of the order of T_K. In nanosized particles, however, the conduction states have discrete energy levels and the energy spacing leads to an additional energy scale that competes with the Kondo temperature. A small heavy-fermion particle is considered, described by the Anderson model in the $U\to\infty$ limit, so that only two electronic configurations—namely, f^0 and f^1—are allowed. A mean-field approximation with one slave boson per *f* site is used to study the susceptibility, the entropy, and the specific heat at low temperatures. All quantities increase rapidly with *T* as a consequence of exponential activations due to the discreteness of the energy spectrum until the heavy-electron state is formed. The possibility of ferromagnetic order is investigated using the formulation of Kotliar and Ruckenstein in terms of three auxiliary bosons per site. The mean-field approximation yields several possible magnetic phases for the ground state as a function of the *f*-level position. In the strongly mixed-valent regime the transition from the paramagnetic to the ferromagnetic phase is signaled as a function of temperature by a diverging susceptibility. It is concluded that the thermal and magnetic properties of very small heavy-fermion particles are quite different from those of bulk heavy-fermion material.

DOI: 10.1103/PhysRevB.65.024431 PACS number(s): 75.20.Hr, 75.30.Mb, 75.75.+a, 73.22.−f

I. INTRODUCTION

Heavy-fermion systems at low temperatures and as a function of magnetic field, pressure, or alloying may show a variety of phenomena, such as unconventional superconductivity, antiferromagnetism, ferromagnetism, quadrupolar order, non-Fermi-liquid properties, or just enhanced paramagnetism, all believed to arise from the band of heavy electrons. The origin of heavy electrons is the competition and interplay of strong local atomiclike Coulomb forces with the solid-state effects of the conduction band and the hybridization, which give rise to a $4f$ or $5f$ Kondo-like resonance at the Fermi level.

In small metallic clusters the spacing of the energy states is determined by the finite size of the system. The discreteness of the energy spectrum has dramatic consequences on the low-temperature properties.[1] For a spherical metallic particle the electron states are described by a shell model.[2] Possible choices of the confining potential are the three-dimensional harmonic potential, the infinite square well, or interpolations thereof, all yielding similar results: i.e., discrete energy levels. For the infinite square well the wave function is given by the product of a spherical Bessel function and a spherical harmonic. The condition that the wave function vanish at an infinite wall yields the relation $j_l(k_n^{(l)}R)=0$, where *R* is the radius of the sphere, *l* is the angular momentum, and $n=1,2,\ldots$ labels the zeros of the Bessel function in increasing order. The energy of the states is then given by $E_{l,n}=(\hbar k_n^{(l)})^2/(2m^*)$, with m^* being the effective mass. Due to the spherical symmetry, the energy does not depend on the quantum number for the projection of the angular momentum m_z, but this degeneracy is lifted for other shapes or symmetries. With increasing energy the sequence of states is then $1s$, $1p$, $1d$, $2s$, $1f$, $2p$, etc., with the degeneracy given by the orbital and spin angular momenta. The shell model gives rise to *magic numbers* when a shell is filled, which has been verified experimentally.[1] The energy spacing is proportional to R^{-2} (for the infinite square well) and decreases rapidly in the macroscopic limit. For nanoscales the discreteness of the levels is a fundamental property.

In this paper we study the low-temperature behavior of a nanosized heavy-electron system. The main difference with the standard heavy-fermion lattice is that the energy spectrum of the conducting states is now discrete. The physics involved is not expected to be very sensitive to the details of this discrete spectrum, so that for simplicity we choose the levels as nondegenerate (except for the spin) and with equal energy spacings. We assume that the correlated localized states correspond to the $4f^0$ and $4f^1$ configurations (e.g., Ce ions or alternately Yb ions if electrons and holes are interchanged) with the energy of the *f* level independent of the position of the ion within the particle. In principle, the *f*-level energy and the valence of the rare-earth ions are expected to be somewhat different for atoms close to the surface of the cluster. In other words, for simplicity we neglect these surface effects and assume in addition that the hybridization between the correlated *f* states and the conduction states is the same at every site. Due to the low crystalline field symmetry, we assume that the $4f^1$ states can be characterized by a doublet. The Hamiltonian of the system is then

$$H=\sum_{i\sigma}\epsilon_i c_{i\sigma}^{\dagger}c_{i\sigma}+\epsilon_f\sum_{l\sigma}|l\sigma\rangle\langle l\sigma| + V\sum_{l\sigma}(c_{l\sigma}^{\dagger}|l0\rangle\langle l\sigma|+|l\sigma\rangle\langle l0|c_{l\sigma}), \quad (1)$$

where i and l label the conduction states and the rare-earth sites in the cluster, respectively. Here $|l\sigma\rangle$ denotes a $4f^1$ state of spin σ at the site l and $|l0\rangle$ the corresponding $4f^0$ state. The f states satisfy at every site the completeness condition

$$\sum_{\sigma} |l\sigma\rangle\langle l\sigma| + |l0\rangle\langle l0| = 1. \tag{2}$$

The two sets of basis states $\{i\}$ and $\{l\}$ are orthonormal and related to each other by a unitary transformation $\tilde{U}$. The many-body aspect of the problem is hidden in the commutation relations of the bra and ket states, which represent correlated electrons ($U \to \infty$) and are not free fermions.

In Sec. II we rewrite the Hamiltonian in terms of one slave boson per site.[3] Slave bosons correspond to an exact reformulation of the problem and are very suitable for a mean-field treatment of the correlations. In particular, the single-slave-boson approach provides an adequate description of the paramagnetic phase. We discuss the low-temperature entropy, specific heat, and magnetic susceptibility, which show an exponential activation due to the discreteness of the energy spectrum. The energy eigenvalues are renormalized by the hybridization and the slave bosons, and this energy spacing is much smaller than that of the host. At temperatures higher than the spacing the heavy-electron state is recovered. In Sec. III we reinvestigate the problem within a three-auxiliary-boson approach. The slave bosons act as projectors onto the respective states of the $4f^0$ and $4f^1$ configurations. Within the mean-field approximation we study the possibility of magnetic order. Due to the discreteness of the energy spectrum, the spin-up and spin-down levels can individually be pulled through the Fermi level, so that numerous magnetic phases (in addition to the paramagnetic one) can be obtained as a function of ϵ_f. The transition from the paramagnetic phase to the first magnetically ordered phase is also studied as a function of temperature. Conclusions are presented in Sec. IV.

The Kondo effect in an ultrasmall metallic grain has been studied previously using the noncrossing diagram approximation within the framework of an Anderson impurity.[4] It was found that the Kondo resonance is strongly affected when the mean level spacing is comparable to T_K and it also depends on the parity of the number of electrons. An Anderson-like impurity model in a finite-size system was also studied by Buttiker and Stafford[5] in the context of tunneling into a quantum dot embedded or as a side branch to a small metallic ring. These situations refer to impurities in nanoscale particles, whereas in the present paper we study a small heavy-fermion particle: i.e., the analog of the Anderson lattice in a large system.

Exponential activations of thermodynamic and transport properties are also observed in so-called Kondo insulators. The indirect narrow gap in these semiconductors arises from the coherent hybridization of the f levels with the conduction states. The gap is of the order of T_K and essentially independent of the system size. Its origin and nature are entirely different from the finite-size gaps in a nanoscale metallic particle. Kondo insulators have been intensively studied with the same methods employed in this paper.[6,7]

II. PARAMAGNETIC PHASE

A. Single-slave-boson formulation

We introduce slave-boson creation and annihilation operators[3] $b_l^\dagger$ and b_l, which act as projectors onto the $4f^0$ configuration at site l, and fermion operators for the $4f^1$ states at site l, $f_{l\sigma}^\dagger$, and $f_{l\sigma}$. The completeness relation equivalent to the condition (2) is now[3]

$$\sum_{\sigma} f_{l\sigma}^\dagger f_{l\sigma} + b_l^\dagger b_l = 1. \tag{3}$$

Transitions between configurations are described by the operators $|l0\rangle\langle l\sigma| = b_l^\dagger f_{l\sigma}$. The Hamiltonian in auxiliary space is given by

$$H_b = \sum_{i\sigma} \epsilon_i c_{i\sigma}^\dagger c_{i\sigma} + \epsilon_f \sum_{l\sigma} f_{l\sigma}^\dagger f_{l\sigma} + V \sum_{l\sigma} (c_{l\sigma}^\dagger b_l^\dagger f_{l\sigma} + f_{l\sigma}^\dagger b_{l\sigma} c_{l\sigma}), \tag{4}$$

subject to the constraint (3), which restricts the model to the physical subspace. The above slave-boson formulation is exact; i.e., it does not contain approximations with respect to the original Hamiltonian (1).

B. Mean-field approximation

We now study Hamiltonian (4) subject to the constraint (3) in the mean-field approximation. The mean-field approximation for the slave-boson formulation has given reliable results for several many-body systems, e.g., the degenerate Anderson model (mixed-valent Ce and Yb ions) for the single-impurity,[8] the two-impurity,[9] and the Anderson lattice[9,10] problems. The auxiliary boson saddle-point approximation is related to a $1/N_f$ expansion, where N_f is the degeneracy of the localized states. In particular, the mean-field solution of the Anderson impurity problem was found to be in good quantitative agreement with the exact Bethe ansatz solution even for relatively small degeneracies.[11] A similarly good quantitative agreement with the exact Bethe ansatz solution was obtained for an isolated Mn impurity embedded into a spin-polarized lattice and for the general case with the noncrossing diagram approximation (see Ref. 12). The correct sequence of magnetic phases was also obtained for manganites within this approach.[13] From the above examples it is known that the mean-field approximation may introduce spurious phase transitions as a function of temperature, but does provide reliable results for the ground state in the absence of large degeneracy lifting fields. It is then expected that the slave boson mean-field approach will also render reliable results for a nanoscale heavy-fermion particle.

In the mean-field (saddle-point) approximation[8] boson operators are replaced by their expectation values. Assuming that all rare-earth sites have the same valence we have $\langle b_l \rangle = \langle b_l^\dagger \rangle = b$ for all l. The constraint (3) is incorporated via Lagrange multipliers λ_l, which are independent of the site index because all sites are assumed to have the same valence. The Hamiltonian is now bilinear in operators and it is straightforward to rewrite it in the basis $\{i\}$ using the unitary transformation $\tilde{U}$, relating the basis states $\{i\}$ and $\{l\}$. The mean-field Hamiltonian is then diagonal in the index i and has the form

$$H_{mf} = \sum_{i\sigma} \left[\epsilon_i c_{i\sigma}^\dagger c_{i\sigma} + (\epsilon_f - \lambda) f_{i\sigma}^\dagger f_{i\sigma} + Vb(f_{i\sigma}^\dagger c_{i\sigma} + c_{i\sigma}^\dagger f_{i\sigma}) \right] + N\lambda(1-b^2), \tag{5}$$

where N is the number of sites.

The mean-field Hamiltonian can be diagonalized for each i and has eigenvalues

$$z_{i\alpha\sigma} = \frac{1}{2}\left[\epsilon_f - \lambda + \epsilon_i + \alpha \sqrt{(\epsilon_f - \lambda - \epsilon_i)^2 + 4b^2V^2} \right], \tag{6}$$

where $\alpha = \pm 1$. Denoting with $d_{i\alpha\sigma}^\dagger$ and $d_{i\alpha\sigma}$ the creation and annihilation operators for the eigenstates we have

$$H_{mf} = \sum_{i\alpha\sigma} z_{i\alpha\sigma} d_{i\alpha\sigma}^\dagger d_{i\alpha\sigma} + N\lambda(1-b^2). \tag{7}$$

The free energy of the system is given by

$$F = -T \sum_{i\alpha\sigma} \ln\{1 + \exp[-(z_{i\alpha\sigma} - \mu)/T]\} + N\lambda(1-b^2) + \mu N_e, \tag{8}$$

where μ is the chemical potential and N_e is the number of electrons.

The minimization of the free energy with respect to b, λ, and μ yields three transcendental equations which self-consistently determine these three parameters,

$$\lambda = \frac{1}{N} \sum_{i\alpha\sigma} \alpha \frac{V^2}{\Delta z_{i\sigma}} f(z_{i\alpha\sigma}),$$

$$1 - b^2 = \frac{1}{N} \sum_{i\alpha\sigma} \alpha \frac{z_{i\alpha\sigma} - \epsilon_i}{\Delta z_{i\sigma}} f(z_{i\alpha\sigma}),$$

$$N_e = \sum_{i\alpha\sigma} f(z_{i\alpha\sigma}), \tag{9}$$

where $f(z_{i\alpha\sigma})$ denotes the Fermi function and $\Delta z_{i\sigma} = \sqrt{(\epsilon_f - \lambda - \epsilon_i)^2 + 4b^2V^2}$ is the difference between $z_{i\alpha\sigma}$ with $\alpha = +1$ and $\alpha = -1$.

The strategy used to solve these equations is the following. Note that the second and third equations only depend on $\epsilon_f - \lambda$ but not on these parameters separately. The first equation can then be used to determine ϵ_f as a function of b, $\epsilon_f - \lambda$, and μ. The third equation determines the chemical potential for fixed b and $\epsilon_f - \lambda$. We then vary b for given $\epsilon_f - \lambda$ (adjusting μ for each case) until the second equation is satisfied. As mentioned above the first equation then determines ϵ_f and λ as a function of $\epsilon_f - \lambda$.

C. Results

The above equations considerably simplify for the ground state, because the Fermi functions are either equal to 0 or 1. We assume that the number of electrons, N_e, is smaller than $2N$, so that the states of the upper band with energies $z_{i\alpha\sigma}$ for $\alpha = +1$ are not occupied. Depending on whether N_e is even or odd the ground state is a singlet or doubly degenerate. We limit ourselves to discuss the situation of even N_e. The spectrum is discrete so that the Fermi level then lies between energy levels. The level spacing in the neighborhood of the Fermi level for N_e close to $2N$ is much smaller than that of the conduction states, as a consequence of the relatively small effective hybridization Vb. This strongly reduced energy gap is the precursor to the heavy-fermion state. Consequently, the entropy and the specific heat are exponentially activated (Arrhenius law involving this reduced gap) at very low temperatures.

For the ground-state magnetization we have to distinguish two situations. In general there are two gyromagnetic factors involved: namely, g_e for the extended states and g_f for the f states. If $g_e = g_f$, spin conservation implies that also the magnetization is a conserved quantity, so that the zero-field susceptibility is zero. As a function of temperature the susceptibility is exponentially activated, similarly to the specific heat. If $g_e \neq g_f$, on the other hand, the magnetization is not conserved and the ground-state susceptibility is finite. The finite χ arises from van Vleck admixtures of excited states into the ground state as a function of field. In the Kondo limit the van Vleck susceptibility is in general rather small and below we limit ourselves to discuss the situation $g_e = g_f$.

The entropy is obtained by differentiating the free energy with respect to T. The free energy has an explicit and implicit temperature dependence, the latter through the self-consistently determined parameters b, λ, and μ. However, since the free energy is minimal with respect to these three parameters, only the explicit dependence needs to be considered. We then have that

$$S = \sum_{i\alpha\sigma} \left\{ \ln\{1 + \exp[-(z_{i\alpha\sigma} - \mu)/T]\} + \frac{z_{i\alpha\sigma} - \mu}{T} f(z_{i\alpha\sigma}) \right\}, \tag{10}$$

which is just the entropy of free fermions with renormalized spectrum $z_{i\alpha\sigma}$. The expression for the specific heat is more involved because now the implicit T dependences of b, λ, and μ have to be considered. It is then more convenient to obtain the specific heat by numerical differentiation of the entropy.

For $g_e = g_f$ the susceptibility is

$$\chi = \frac{1}{4T} \sum_{i\alpha\sigma} \{2 \cosh[(z_{i\alpha\sigma} - \mu)/2T]\}^{-2}, \qquad (11)$$

and is obtained by differentiating F with respect to the field twice. The free energy again has an explicit, the Zeeman splitting, and implicit magnetic field dependences. The derivative of the free energy with respect to the implicit dependence vanishes because F is minimal with respect to b, λ, and μ, and these three quantities are all even functions of the field. The expression (11) then just corresponds to the Zeeman splitting of the energy levels.

In Fig. 1 we present our numerical results for $\epsilon_f = -0.5$, $V = 0.2$, and a spacing of the extended states of $\delta\epsilon = 0.2$, $N = 11$, and $N_e = 18$. The entropy grows monotonically with T, showing the characteristic exponential activation due to the finite size of the system. The dominant gap is much smaller than the level splitting $\delta\epsilon$ of the conduction states. For a large system the characteristic Kondo energy scale (in units of the bandwidth) is given by b^2. For the present example at low T we obtain $b^2 = 0.0882$, which would correspond to a mass enhancement of about 11. The inset shows the entropy at very low T. The specific heat is displayed in Fig. 1(b) for the same parameters and shows an explicit peak structure, which arises from the hybridization gap between the $z_{i\alpha\sigma}$ bands with $\alpha = +1$ and $\alpha = -1$. For $T > 0.005$ the heavy-electron state is already formed, since T is larger than the spacing between levels. The exponential activation at low T is seen in the inset. The susceptibility is presented in Fig. 1(c). On the one hand, the exponential behavior is observed at low T, while, on the other hand, for $T > 0.0004$ the heavy-electron states have already developed—i.e., at a T much lower than is seen in the specific heat. The main difference is that the derivative of the implicit T dependence of b, λ, and μ enters the specific heat, but not the susceptibility.

The same quantities are shown in Fig. 2 for the same set of parameters except that $\epsilon_f = -1.0$. This gives rise to a smaller Kondo temperature and hence to heavier masses. Here $b^2 = 0.001\,63$, which would correspond to a mass enhancement of 600 in the bulk. The exponential activation at low T is seen in all three quantities, but on a smaller energy scale. The specific heat shows low-T structures for the same reasons as in Fig. 1(b) and also the susceptibility has roughly the same behavior as in Fig. 1(c).

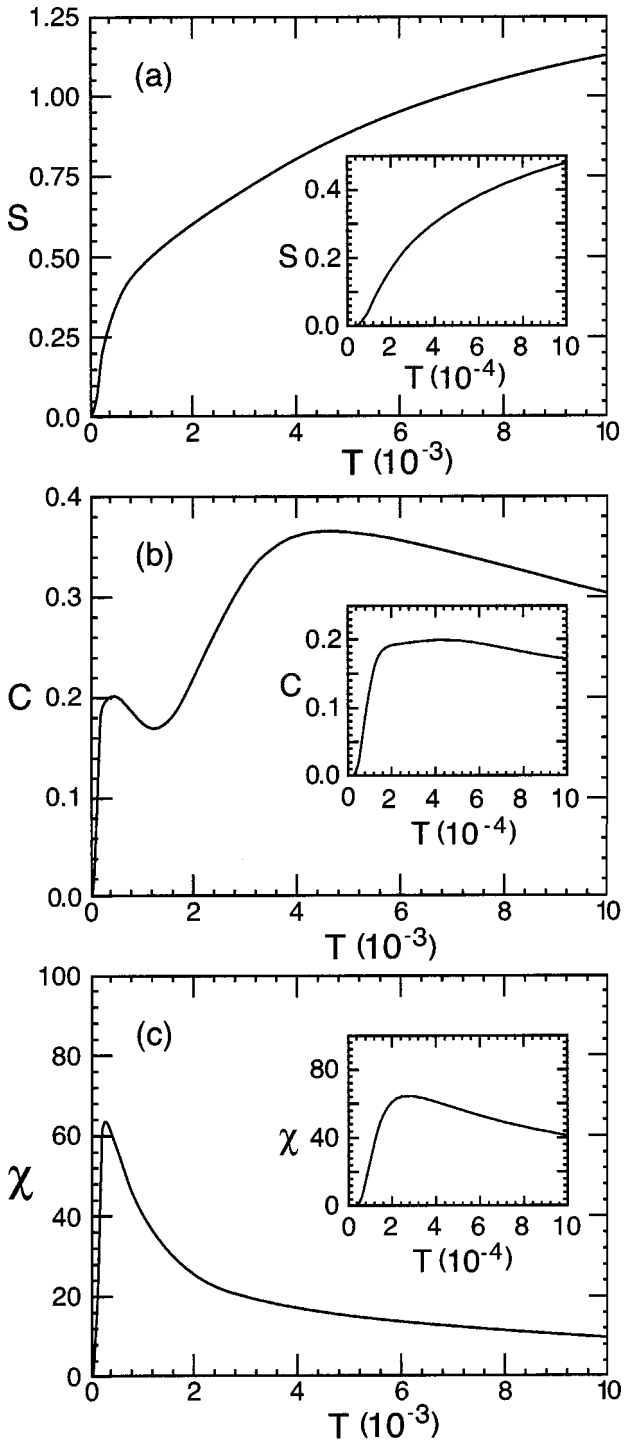

FIG. 1. (a) Entropy, (b) specific heat, and (c) susceptibility as a function of T for the single-slave-boson formulation in a mean field. The curves are for $N_e = 18$, $N = 11$, $V = 0.2$, spacing between energy levels of extended states $\delta\epsilon = 0.2$, and $\epsilon_f = -0.5$. This corresponds to an effective mass enhancement of 11. The insets show the low-temperature behavior.

D. Competition of the level spacing and Kondo temperature

The gaps dominating the low-temperature specific heat and susceptibility are much smaller than the spacing of the energy levels of the host, $\delta\epsilon$. Let us first point out that the spin gap and the charge gap are equal as is expected from a band picture. This is analogous to Kondo insulators (gaps are difficult to measure because of impurity and intrinsic bound states in the gap), but drastically different from impurities (Kondo and Anderson) in nanosized clusters, where the spin gaps dominate the low-T specific heat and susceptibility. In the impurity case, we have to distinguish in addition between spin gaps for spin-singlet (specific heat) and spin-triplet (susceptibility) excitations.

After hybridizing the f states with the conduction states the spacing between the levels (we assume here that the

Fermi level lies between $z_{i\alpha\sigma}$ and $z_{i+1\alpha\sigma}$ with $\alpha=-1$) at the Fermi energy is

$$\delta z_{i\alpha\sigma}=z_{i+1\alpha\sigma}-z_{i\alpha\sigma}\approx\frac{\delta\epsilon}{2}\left[1-\frac{\epsilon_i+\lambda-\epsilon_f}{\Delta z_{i\sigma}}\right]$$

$$\approx\delta\epsilon\,\frac{V^2b^2}{(\epsilon_f-\lambda-\epsilon_i)^2}\approx\delta\epsilon b^2. \tag{12}$$

Hence, the gap of the heavy electrons is reduced by a factor of $b^2\approx T_K/D$ with respect to the original gap of the host. For the example in Fig. 1 (small mass enhancement) the reduction is approximately one order of magnitude, and for the example in Fig. 2 (small T_K) the reduction is about 600 times.

Obviously the low-energy excitation spectrum also depends on the parity of the number of electrons. For an odd number of electrons the ground state is always a doublet and not a singlet as for an even number of electrons in the absence of long-range magnetic order.

III. FERROMAGNETIC PHASES

A. Formulation with three slave bosons per site

In order to study the formation of magnetic phases a different approach with three slave bosons per site has to be employed. The single auxiliary boson projects onto the nonmagnetic $4f^0$ configuration and a mean-field approximation is not favorable to magnetic order. We use here the $U\rightarrow\infty$ variant of Kotliar and Ruckenstein's[14] formulation. Originally the method was conceived to investigate the Hubbard model with finite U with four auxiliary bosons projecting onto the empty, doubly occupied, and singly occupied levels with up and down spin, respectively. This technique was later applied to a model for highly correlated bands of hybridized Cu $3d$ and O $2p$ orbitals[15,16] and the Anderson lattice.[7] The slave-boson approach has also been formulated with spin-rotational invariance,[17] but this does not affect the mean-field results.

In analogy to Ref. 18 we introduce three Bose creation and annihilation operators for each site,[7,14] i.e., $e_l^\dagger, e_l$ for the empty state and $p_{l\sigma}^\dagger, p_{l\sigma}$ for the single occupied states, which act as projectors onto the corresponding electronic states at site l, as well as fermion operators $f_{l\sigma}^\dagger$ and $f_{l\sigma}$. They satisfy the completeness relation and the projector condition

$$e_l^\dagger e_l+p_{l\uparrow}^\dagger p_{l\uparrow}+p_{l\downarrow}^\dagger p_{l\downarrow}=1,$$

$$f_{l\sigma}^\dagger f_{l\sigma}=p_{l\sigma}^\dagger p_{l\sigma}. \tag{13}$$

In physical subspace the operators $|l\sigma\rangle\langle l0|$ and $|l0\rangle\langle l\sigma|$ are replaced by $Z_{l\sigma}^\dagger f_{l\sigma}^\dagger$ and $f_{l\sigma}Z_{l\sigma}$, respectively, so that the matrix elements are invariant in the combined fermion-boson Hilbert space. The definition of the operators $Z_{l\sigma}$ is not unique, and we choose the same expression as in Refs. 7, 14, 18, and 19, i.e.,

$$Z_{l\sigma}=(1-p_{l\sigma}^\dagger p_{l\sigma})^{-1/2}e_l^\dagger p_{l\sigma}(1-e_l^\dagger e_l-p_{l-\sigma}^\dagger p_{l-\sigma})^{-1/2}, \tag{14}$$

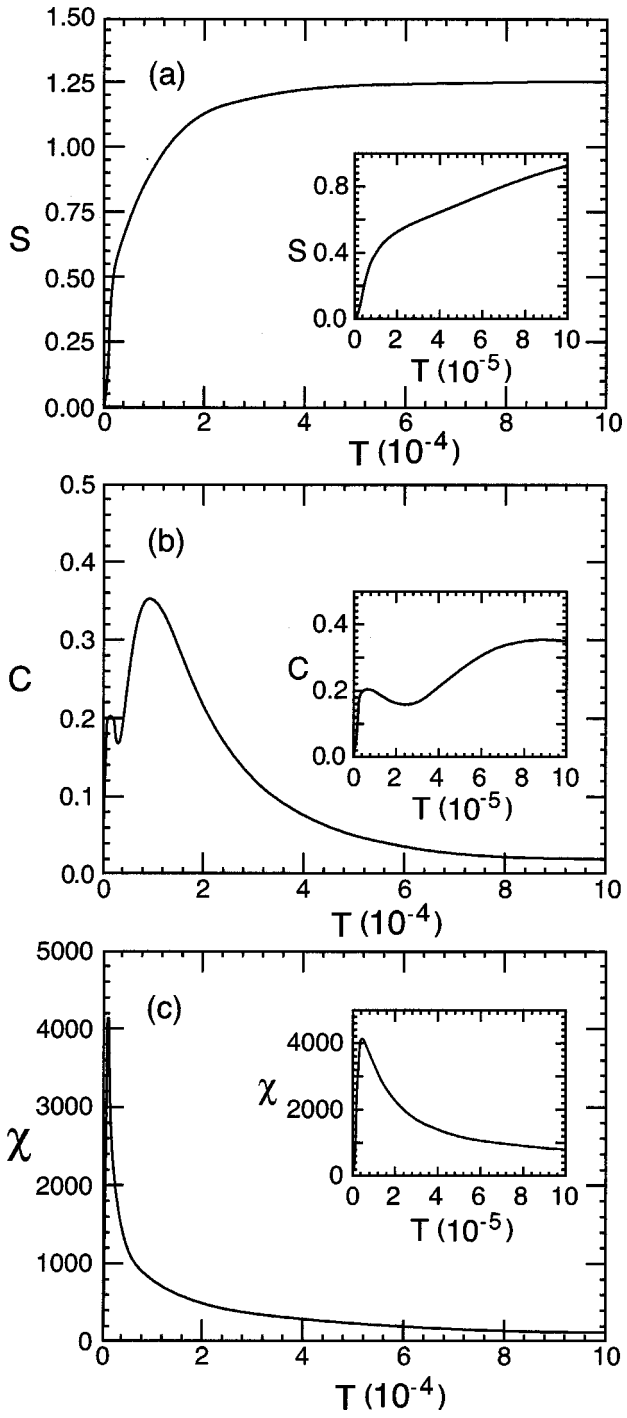

FIG. 2. (a) Entropy, (b) specific heat, and (c) susceptibility as a function of T for the single-slave-boson formulation in a mean field. The curves are for $N_e=18$, $N=11$, $V=0.2$, spacing between energy levels of extended states $\delta\epsilon=0.2$, and $\epsilon_f=-1.0$. This corresponds to an effective mass enhancement of about 600. The insets show the low-temperature behavior.

which yields the correct matrix elements, and for the Hubbard and Anderson models with finite U the correct expectation value of $\langle Z_{l\sigma}^\dagger Z_{l\sigma}\rangle$ within the mean-field approximation as $U\rightarrow 0$.

The constraints, Eqs. (13), are incorporated via Lagrange

multipliers $\lambda_l^{(1)}$ and $\lambda_{l\sigma}^{(2)}$, respectively, and the Hamiltonian in auxiliary space reads

$$H_{sb}=\sum_{i\sigma}\ \epsilon_i c_{i\sigma}^\dagger c_{i\sigma}+\sum_{l\sigma}\ (\epsilon_f+\lambda_{l\sigma}^{(2)})f_{l\sigma}^\dagger f_{l\sigma}$$

$$+V\sum_{l\sigma}\ (c_{l\sigma}^\dagger f_{l\sigma}Z_{l\sigma}+Z_{l\sigma}^\dagger f_{l\sigma}^\dagger c_{l\sigma})$$

$$+\sum_{l}\ \lambda_l^{(1)}(e_l^\dagger e_l+p_{l\uparrow}^\dagger p_{l\uparrow}+p_{l\downarrow}^\dagger p_{l\downarrow}-1)$$

$$-\sum_{l\sigma}\ \lambda_{l\sigma}^{(2)}p_{l\sigma}^\dagger p_{l\sigma}. \tag{15}$$

This slave-boson formulation is exact if confined to the physical subspace; i.e., it does not contain approximations with respect to the original Hamiltonian (1).

B. Mean-field approximation

In the mean-field (saddle-point) approximation we replace all boson operators by their expectation values. We assume that all sites are equivalent, i.e., that the Lagrange parameters do not depend on the index l, and

$$\langle p_{l\sigma}^\dagger\rangle=\langle p_{l\sigma}\rangle=p_\sigma,\quad \langle e_l^\dagger\rangle=\langle e_l\rangle=e,$$

$$\langle Z_{l\sigma}^\dagger\rangle=\langle Z_{l\sigma}\rangle=Z_\sigma. \tag{16}$$

The mean-field Hamiltonian is

$$H_{mf}=\sum_{i\sigma}\ [\epsilon_i c_{i\sigma}^\dagger c_{i\sigma}+(\epsilon_f+\lambda_\sigma^{(2)})f_{i\sigma}^\dagger f_{i\sigma}+VZ_\sigma(f_{i\sigma}^\dagger c_{i\sigma}$$

$$+c_{i\sigma}^\dagger f_{i\sigma})]+N\lambda^{(1)}(e^2-1)+N\sum_\sigma\ (\lambda^{(1)}-\lambda_\sigma^{(2)})p_\sigma^2. \tag{17}$$

Hence the main effect of the Lagrange parameter $\lambda_\sigma^{(2)}$ is to provide a spin-dependent renormalization of the f level, which opens the possibility of magnetic order. Note that as in Eq. (7) the Hamiltonian is bilinear in fermion operators, so that by means of the unitary transformation $\tilde{U}$ it can be expressed in the $\{i\}$ basis.

The diagonalized mean-field Hamiltonian has eigenvalues

$$z_{i\alpha\sigma}=\frac{1}{2}(\epsilon_f+\lambda_\sigma^{(2)}+\epsilon_i)+\frac{1}{2}\alpha\sqrt{(\epsilon_f+\lambda_\sigma^{(2)}-\epsilon_i)^2+4Z_\sigma^2V^2}, \tag{18}$$

where $\alpha=\pm1$, and can be rewritten as

$$H_{mf}=\sum_{i\alpha\sigma}\ z_{i\alpha\sigma}d_{i\alpha\sigma}^\dagger d_{i\alpha\sigma}+N\lambda^{(1)}(e^2-1)$$

$$+N\sum_\sigma\ (\lambda^{(1)}-\lambda_\sigma^{(2)})p_\sigma^2. \tag{19}$$

The free energy is

$$F=-T\sum_{i\alpha\sigma}\ \ln\{1+\exp[-(z_{i\alpha\sigma}-\mu)/T]\}+N\lambda^{(1)}(e^2-1)$$

$$+N\sum_\sigma\ (\lambda^{(1)}-\lambda_\sigma^{(2)})p_\sigma^2+\mu N_e, \tag{20}$$

where N_e is again the number of electrons.

The parameters $\lambda^{(1)}$, $\lambda_\sigma^{(2)}$, p_σ, e, and μ are obtained by minimizing the free energy with respect to these parameters,

$$e^2+p_\uparrow^2+p_\downarrow^2=1,$$

$$p_\sigma^2=\frac{1}{N}\sum_{i\alpha}\ \alpha\ \frac{z_{i\alpha\sigma}-\epsilon_i}{\Delta z_{i\sigma}}f(z_{i\alpha\sigma}),$$

$$\lambda^{(1)}=-\frac{1}{N}\sum_{i\alpha\sigma}\ \alpha\frac{\partial Z_\sigma^2}{\partial e^2}\frac{V^2}{\Delta z_{i\sigma}}f(z_{i\alpha\sigma}),$$

$$\lambda_\sigma^{(2)}-\lambda^{(1)}=\frac{1}{N}\sum_{i\alpha\sigma'}\ \alpha\ \frac{\partial Z_{\sigma'}^2}{\partial p_\sigma^2}\frac{V^2}{\Delta z_{i\sigma'}}f(z_{i\alpha\sigma'}),$$

$$N_e=\sum_{i\alpha\sigma}\ f(z_{i\alpha\sigma}), \tag{21}$$

where now $\Delta z_{i\sigma}=\sqrt{(\epsilon_f+\lambda_\sigma^{(2)}-\epsilon_i)^2+4Z_\sigma^2V^2}$. Defining $p_\sigma^2=p_0^2+\sigma m$ and $\lambda_\sigma^{(2)}=\lambda_0^{(2)}+\sigma\epsilon_m$ with $\sigma=\pm\frac{1}{2}$, the second and fourth equations can be rewritten as

$$p_0^2=\frac{1}{2N}\sum_{i\alpha\sigma}\ \alpha\ \frac{z_{i\alpha\sigma}-\epsilon_i}{\Delta z_{i\sigma}}f(z_{i\alpha\sigma}),$$

$$m=\frac{2}{N}\sum_{i\alpha\sigma}\ \alpha\sigma\ \frac{z_{i\alpha\sigma}-\epsilon_i}{\Delta z_{i\sigma}}f(z_{i\alpha\sigma}),$$

$$\lambda_0^{(2)}=-\frac{1}{2N}\sum_{i\alpha\sigma}\ \alpha\frac{1-2\sigma m}{(1-p_\sigma^2)^2}\frac{V^2}{\Delta z_{i\sigma}}f(z_{i\alpha\sigma}),$$

$$\epsilon_m=\frac{2}{N}\sum_{i\alpha\sigma}\ \alpha\sigma\frac{e^2}{(1-p_\sigma^2)^2}\frac{V^2}{\Delta z_{i\sigma}}f(z_{i\alpha\sigma}). \tag{22}$$

All equations except the third of Eqs. (22) depend only on $\epsilon_f+\lambda_0^{(2)}$, so that this equation can be used to determine ϵ_f once all other parameters are known. Note that $\lambda^{(1)}$ does not enter physical quantities. There are then five equations to be solved self-consistently.

C. Magnetic phases in the ground state

A magnetic phase is characterized by a nonzero magnetization m and a nonzero spin-dependent f-level energy shift ϵ_m. We then search for nontrivial solutions of the second and fourth equations of the set (22). For simplicity we limit ourselves to the ground state, where the magnetic order is expected to be most pronounced. At $T=0$ the Fermi functions are either 0 or 1, which considerably simplifies the calculation. If there is more than one solution of the equations for

the same parameters ϵ_f and V, then their energy has to be compared to see which state is the ground state. The ground-state energy is given by

$$E_{GS}=\sum_{i\alpha\sigma} z_{i\alpha\sigma} f(z_{i\alpha\sigma})-N(p_\uparrow^2\lambda_\uparrow^{(2)}+p_\downarrow^2\lambda_\downarrow^{(2)}). \qquad (23)$$

Note that the explicit dependence on the chemical potential and $\lambda^{(1)}$ has canceled out.

The system of equations always has a paramagnetic solution for which $m=0$ and $\epsilon_m=0$. As a function of ϵ_f the number of f electrons decreases monotonically, from $n_f=2p_0^2$ approximately 1 to asymptotically 0. For large values of ϵ_f the paramagnetic is the only solution, because p_0^2 is not large enough to induce magnetic order in the f band (mixed valence regime). Note that the paramagnetic phase is meaningless for very negative ϵ_f, because it corresponds to $p_0^2=0.5$, i.e., $e^2=0$.

As n_f increases with decreasing ϵ_f, the discrete levels near to the Fermi level are closer spaced. Under these circumstances magnetic solutions are possible. They correspond to filling one more up-spin level at the expense of a down-spin level. If ϵ_f is lowered further, several such solutions may exist; i.e., two or more levels are displaced with respect to the paramagnetic solution. The solutions for p_σ^2 are presented in Fig. 3(a). For the present set of parameters ($V=0.2$, $\delta\epsilon=0.2$, $N=11$, and $N_e=18$) there are four ferromagnetic phases in addition to the paramagnetic one. They exist only over a limited range of ϵ_f. The energy corresponding to these five phases is displayed in Fig. 3(b). Several level crosses and transitions are observed. All transitions involve a jump in the magnetization. A distinction between first- and second-order transitions does of course not make sense in a nanoscale system. Also for a nanosized particle the ground-state energy may have discontinuities. With decreasing ϵ_f the sequence of ground-state phases is then from paramagnetic (P) to F1 to F2 to P to F3 to P to F4. This phase diagram refers to this specific nanoparticle, but similar results are expected for other parameters.

In the limit of a large system (thermodynamic limit) the present approach is closely related to Gutzwiller's variational ansatz,[18,20,21] which has been studied as a function of the orbital degeneracy L. The $L=0$ case is the most favorable for ferromagnetism and with increasing L the onset of the magnetic instability is pushed towards lower values of ϵ_f. Also the characteristic energy scale of the paramagnetic phase—i.e., the Kondo temperature—is different from the traditional T_K of the single-impurity model. Although $\ln(T_K/D)$, where D is the bandwidth, is proportional to the inverse of the exchange coupling, the dependence on the degeneracy is different. This has originally been attributed to a "lattice enhancement of the Kondo effect,"[20] but is now believed to be an artifact of the Gutzwiller approximation.

D. Susceptibility

In this subsection we investigate the low-temperature entropy and susceptibility in the paramagnetic phase. The entropy is obtained by differentiating the free energy with respect to the temperature. Since the free energy is minimal with respect to variational parameters, only the explicit dependence on T enters and the entropy is just the one of free fermions with spectrum $z_{i\alpha\sigma}$ as given by Eq. (10). The specific heat is then obtained by numerical differentiation of the entropy. At low T these quantities follow an exponential activation as for the situation studied in Sec. II.

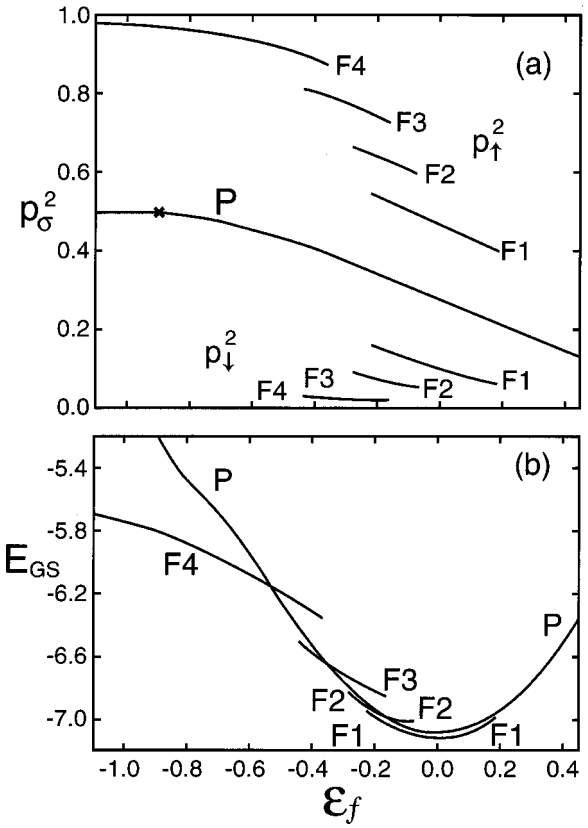

FIG. 3. Solution of the self-consistent mean-field equations for the three auxiliary boson formulation at $T=0$ for $N_e=18$, $N=11$, $V=0.2$, and spacing between energy levels of extended states $\delta\epsilon=0.2$. Shown is (a) the f-level population for up and down spins and (b) the energy for the different phases as a function of ϵ_f. For the present example a paramagnetic (P) solution and four ferromagnetic ones (F1, F2, F3, and F4) are found. As a function of ϵ_f the ground state changes several times between the paramagnetic and ferromagnetic phases.

The susceptibility in the P phase as a function of T and ϵ_f is an interesting quantity, because it indicates the onset of magnetic order with a divergence. Although long-range order is a concept not compatible with nanoscale particles, we can formally expand the free energy close to a transition in powers of the magnetization m and ϵ_m, as in a Ginzburg-Landau functional. Mean-field exponents are exact in this case. The leading term is quadratic in these quantities. The transition to the F1 phase (divergence of χ) is then signaled by the vanishing of a determinant. Rather than expanding the free energy, it is more convenient to expand the magnetization. The result is presented in the Appendix. Note that the expression of the susceptibility, Eq. (A1), is different from Eq. (11). The reason for this difference is the fact that two of the three

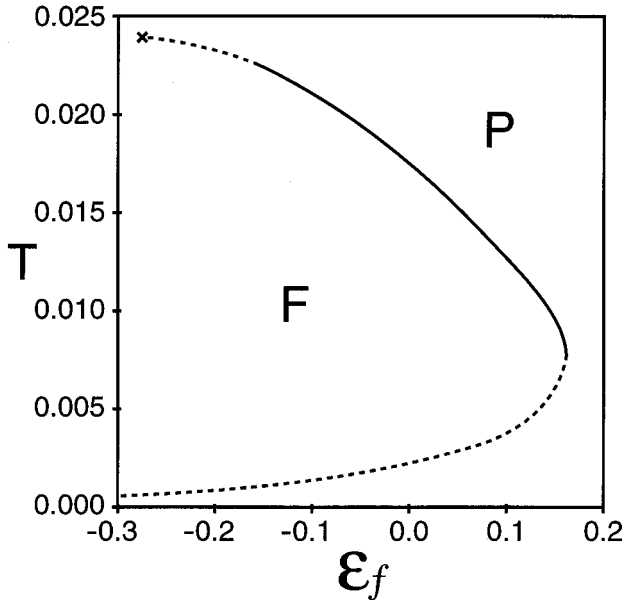

FIG. 4. Transition temperature from the paramagnetic to ferromagnetic phases as a function of ϵ_f. Only a continuous transition is considered. The determinant of Eq. (A5) also vanishes along the lower branch, but this solution does not correspond to a physical situation, because the ferromagnetic phase is stable in that region. The cross denotes the end point of the upper branch, but a discontinuous transition is believed to set in already before reaching this point. Parameters as in Fig. 3.

auxiliary bosons, as well as $\lambda_\sigma^{(2)}$, have a nontrivial field dependence, in contrast to the one-slave-boson approach of Sec. II.

The necessary condition for a diverging susceptibility is that the determinant associated with the 2×2 system of Eqs. (A5) vanishes. The result for this condition in the T-ϵ_f plane is shown in Fig. 4. The susceptibility refers to the paramagnetic phase and this expansion only is meaningful if the magnetization disappears continuously at the P-F boundary; i.e., if the magnetization jumps to zero, χ does not diverge. This is believed to happen for ϵ_f less than -0.15 in Fig. 4. The cross indicates the point where χ no longer diverges. The lower branch of the $T(\epsilon_f)$ curve does not have physical significance, because it takes place in the region where the F1 or F2 phases are the stable ones.

The remainder of the phase diagram at finite T is rather tedious to obtain because the magnetization is expected to have several discontinuous transitions until it reaches the paramagnetic state. Moreover, the many-slave-boson approaches usually overemphasize the phases with magnetic order, since the mean field suppresses quantum and thermal fluctuations. It is then difficult to get a reliable finite-T phase diagram without using in addition other criteria.

IV. CONCLUSIONS

We studied the low-temperature and magnetic properties of a nanosized heavy-fermion particle described in terms of the Anderson model. For simplicity we have neglected surface effects, although it is believed that atoms close to the boundary of the particle will have different model parameters. There are two main differences between a nanoparticle and the infinite lattice. First, the electronic energy levels are discrete; i.e., they have finite spacing which depends on the size of the particle. Consequently the low-T properties are exponentially activated. This feature is not qualitatively changed by surface effects. Second, the results depend on the parity of N_e. If N_e is odd, the ground state is doubly degenerate. In this paper we limit ourselves to even N_e.

We employed two different mean-field auxiliary boson approaches to incorporate the local correlations in the f shells. In Sec. II a single-slave-boson operator per site was introduced, which acts as a projector onto the $4f^0$ configuration. In the continuum limit this approach reproduces the correct Kondo energy scale and provides a good qualitative description of the low-T heavy-fermion lattice.[9,10] We studied the entropy, specific heat, and susceptibility at low and intermediate T. The specific heat displays structure due to the hybridization gap, which is close to the Fermi level of the heavy electrons. The crossover from exponential activation to the heavy-electron state occurs at quite low T in the susceptibility.

The exponential activation at low T in the susceptibility and the specific heat corresponds to the same gap. This gap is reduced with respect to the energy-level spacing in the host by a factor $b^2=T_K/D$, as a consequence of the ''mass enhancement.'' The interplay of the Kondo temperature with the mean-level spacing in the host yields then a new energy scale. This contrasts the behavior of an isolated impurity embedded into a metallic nanoparticle for which the spin and charge gaps are renormalized differently.

The mean-field approximation of the single-slave-boson formulation always favors the paramagnetic phase. To investigate possible ferromagnetic phases we have to introduce as well projectors onto the states of the $4f^1$ configuration. On the lattice—i.e., in the thermodynamic limit—this approach[14] is equivalent to Gutzwiller's approximation,[20,21] which yields a characteristic energy scale different from the traditional Kondo temperature.[18,20] This approach tends to overestimate magnetic order. We obtain several ferromagnetic phases, which are associated with the crossing of the Fermi level by individual levels. As a function of the f-level energy a rich ground-state phase diagram is obtained this way. The transition from the paramagnetic to the first ferromagnetic state is signaled by a diverging susceptibility at the transition temperature. However, most transitions between phases are discontinuous. In the thermodynamic limit, also a discontinuous transition from the paramagnetic to ferromagnetic ground state is obtained when ϵ_f is lowered.[18]

For simplicitly we have limited ourselves to study a relatively small metallic particle. However, we do not expect qualitative changes to occur with increasing size of the cluster, so that the formation of the heavy-fermion state can be studied as a function of the size of the particle. It would also be interesting to experimentally investigate these nanoparticles via electron spin resonance in or close to the ferromagnetic phases. The electromagnetic field induces spin flips, which correspond to transitions between the different ferro-

magnetic states. An advantage of the small size is that magnon relaxation is very limited, so that the ESR linewidths are expected to be narrow and the resonances well defined.

Finally, we would like to address the validity of the mean-field approaches. At the beginning of Sec. II B we listed some models that have successfully been solved using the single-slave-boson formulation.[8–13] Here the criteria to determine success are comparisons with results from other methods, e.g., the Bethe ansatz for integrable impurity models and approximate methods such as the noncrossing diagram approximation (NCA), diagram summations, etc. It is more difficult to determine the reliability of the mean field in the three-slave-boson formulation, but similar variants have been applied to numerous other problems,[14–17] including Kondo insulators.[7] Fluctuations, neglected in the mean-field approach, are less controlled in finite-size systems and it is hard to provide a quantitative estimate of the error. However, based on the previous experience with slave-boson mean-field approaches, we expect our results to be correct not only qualitatively, but also quantitatively reliable.

ACKNOWLEDGMENTS

The support by the National Science Foundation under Grants No. DMR98-01751 and DMR01-05431 and the Department of Energy under Grant No. DE-FG02-98ER45797 is acknowledged.

APPENDIX

In the paramagnetic phase the magnetization is obtained by differentiating the free energy with respect to the external magnetic field. We consider here the situation $g_e=g_f$ for which the magnetization is a conserved quantity, $M=\Sigma_{i\alpha\sigma}\sigma f(z_{i\alpha\sigma}-\sigma H)$. The zero-field susceptibility is now given by

$$\chi=\frac{1}{T}\sum_{i\alpha\sigma}\frac{\sigma^2-\sigma\partial z_{i\alpha\sigma}/\partial H}{\{2\cosh[(z_{i\alpha\sigma}-\mu)/2T]\}^2}, \tag{A1}$$

where $\partial\mu/\partial H$ is zero because μ is even in H. It is straightforward to see that

$$\frac{\partial z_{i\alpha\sigma}}{\partial H}=\alpha\frac{z_{i\alpha\sigma}-\epsilon_i}{\Delta z_{i\sigma}}\frac{\partial\lambda_\sigma^{(2)}}{\partial H}+\alpha\frac{2V^2}{\Delta z_{i\sigma}}\frac{e^2}{(1-p_\sigma^2)^2}\frac{\partial p_\sigma^2}{\partial H}, \tag{A2}$$

where we used the fact that e^2 is even in the field, but $\lambda_\sigma^{(2)}$ and p_σ^2 have a linear component in H, which is obtained by differentiating the second and fourth of Eqs. (21) with respect to the field.

Defining

$$A_1=\frac{1}{N}\sum_{i\alpha}\alpha\frac{f(z_{i\alpha\sigma})}{\Delta z_{i\sigma}},$$

$$A_2=\frac{1}{N}\sum_{i\alpha}\alpha\frac{f(z_{i\alpha\sigma})}{(\Delta z_{i\sigma})^3},$$

$$A_3=\frac{1}{N}\sum_{i\alpha}\alpha\frac{f(z_{i\alpha\sigma})}{(\Delta z_{i\sigma})^3}\sum_{\alpha'}[z_{i\alpha'\sigma}-\epsilon_i],$$

$$A_4=\frac{1}{N}\sum_{i\alpha}\alpha\frac{f(z_{i\alpha\sigma})}{(\Delta z_{i\sigma})^3}\prod_{\alpha'}[z_{i\alpha'\sigma}-\epsilon_i], \tag{A3}$$

and

$$B_1=\frac{1}{N}\sum_{i\alpha}\alpha\frac{ch(z_{i\alpha\sigma})}{\Delta z_{i\sigma}},$$

$$B_2=\frac{1}{N}\sum_{i\alpha}\frac{ch(z_{i\alpha\sigma})}{(\Delta z_{i\sigma})^2},$$

$$B_3=\frac{1}{N}\sum_{i\alpha}\frac{(z_{i\alpha\sigma}-\epsilon_i)ch(z_{i\alpha\sigma})}{(\Delta z_{i\sigma})^2},$$

$$B_4=\frac{1}{N}\sum_{i\alpha}\alpha\frac{(z_{i\alpha\sigma}-\epsilon_i)ch(z_{i\alpha\sigma})}{\Delta z_{i\sigma}},$$

$$B_5=\frac{1}{N}\sum_{i\alpha}\frac{(z_{i\alpha\sigma}-\epsilon_i)^2ch(z_{i\alpha\sigma})}{(\Delta z_{i\sigma})^2}, \tag{A4}$$

where $ch(z_{i\alpha\sigma})=\{2\cosh[(z_{i\alpha\sigma}-\mu)/2T]\}^{-2}$, we have with $X=V^2e^2/(1-p_\sigma^2)^2$

$$\frac{\partial\lambda_\sigma^{(2)}}{\partial H}=\sigma X\frac{B_1}{T}-X\left(A_3+\frac{B_3}{T}\right)\frac{\partial\lambda_\sigma^{(2)}}{\partial H}+\left[\frac{2XA_1}{(1-p_\sigma^2)}-X^2\left(2A_2+\frac{B_2}{T}\right)\right]\frac{\partial p_\sigma^2}{\partial H},$$

$$\frac{\partial p_\sigma^2}{\partial H}=\sigma\frac{B_4}{T}-\left(2A_4+\frac{B_5}{T}\right)\frac{\partial\lambda_\sigma^{(2)}}{\partial H}-X\left(A_3+\frac{B_3}{T}\right)\frac{\partial p_\sigma^2}{\partial H}. \tag{A5}$$

The solution of this system of two equations with two unknowns ($\partial p_\sigma^2/\partial H$ and $\partial\lambda_\sigma^{(2)}/\partial H$) yields the susceptibility. The necessary condition for a divergent susceptibility is that the determinant vanish.

[1] W.A. de Heer, Rev. Mod. Phys. **65**, 611 (1993); M. Brack, *ibid.* **65**, 677 (1993).
[2] M. Göppert-Mayer and J.H.D. Jensen, *Elementary Theory of Nuclear Shell Structure* (Wiley, New York, 1953).
[3] S.E. Barnes, J. Phys. F: Met. Phys. **6**, 1375 (1976); P. Coleman, Phys. Rev. B **29**, 3035 (1984).
[4] W.B. Thimm, J. Kroha, and J. von Delft, Phys. Rev. Lett. **82**, 2143 (1999).
[5] M. Buttiker and C.A. Stafford, Phys. Rev. Lett. **76**, 495 (1996).
[6] P. Schlottmann, Phys. Rev. B **46**, 998 (1992).
[7] V. Dorin and P. Schlottmann, Phys. Rev. B **46**, 10 800 (1992).
[8] N. Read and D.M. Newns, J. Phys. C **16**, L1055 (1983); P. Cole-

man, J. Magn. Magn. Mater. **47**, 323 (1985).
[9] P. Coleman, in *Theory of Heavy-Fermions and Valence Fluctuations*, edited by T. Kasuya and T. Saso (Springer-Verlag, New York, 1985), p. 163.
[10] A.J. Millis and P.A. Lee, Phys. Rev. B **35**, 3394 (1987); A. Auerbach and K. Levin, Phys. Rev. Lett. **57**, 877 (1986).
[11] J.W. Rasul and A.C. Hewson, J. Phys. C **17**, 3337 (1984).
[12] P. Schlottmann, Phys. Rev. B **58**, 3160 (1998).
[13] P. Schlottmann, Phys. Rev. B **62**, 439 (2000).
[14] G. Kotliar and A.E. Ruckenstein, Phys. Rev. Lett. **57**, 1362 (1986).
[15] C.A. Balseiro, M. Avignon, A.G. Rojo, and B. Alascio, Phys. Rev. Lett. **62**, 2624 (1989).
[16] A. Sudbo and A. Houghton, Phys. Rev. B **42**, 4105 (1990).
[17] T. Li, P. Wölfle, and P.J. Hirschfeld, Phys. Rev. B **40**, 6817 (1989).
[18] V. Dorin and P. Schlottmann, J. Appl. Phys. **73**, 5400 (1993).
[19] V. Dorin and P. Schlottmann, Phys. Rev. B **47**, 5095 (1993).
[20] T.M. Rice and K. Ueda, Phys. Rev. Lett. **55**, 995 (1985).
[21] P. Fazekas and E. Müller-Hartmann, Z. Phys. B: Condens. Matter **85**, 285 (1991).